Tech Science Press

Mechanical Properties and Stress Strain Relationship Models for Bamboo Scrimber

Haitao Li[1,*], Huizhong Zhang[1], Zhenyu Qiu[1], Jingwen Su[2], Dongdong Wei[3], Rodolfo Lorenzo[4], Conggan Yuan[3], Hongzheng Liu[5] and Chungui Zhou[6]

[1]College of Civil Engineering, Nanjing Forestry University, Nanjing, 210037, China
[2]Nanjing Technical Vocational College, Nanjing, 210019, China
[3]Jiangxi Feiyu Bamboo Stock Co. Ltd., Fengxin, 330700, China
[4]University College London, London, WC1E 6BT, UK
[5]Hangzhou Dasuo Technology Co. Ltd., Hangzhou, 311251, China
[6]Hangzhou Runzhu Technology Co. Ltd., Hangzhou, 311200, China
*Corresponding Author: Haitao Li. Email: lhaitao1982@126.com

Abstract: In order to investigate the basic mechanical properties and stress strain relationship model for bamboo scrimber manufactured based on a new technique, a large quantities of experiments have been carried out. Based on the analysis of the test results, the following conclusions can be drawn. Two main typical failure modes were classified for bamboo scrimber specimens both under tension parallel to grain and tension perpendicular to grain. Brittle failure happened for all tensile tests. The slope values for the elastic stages have bigger discreteness compared with those for the specimens under tensile parallel to grain. The failure modes for bamboo scrimber specimens under compression parallel to grain could be divided into four. Only one main failure mode happened both for the bending specimens and the shear specimens. With the COV values of 28.64 and 25.72 respectively, the values for the strength and elastic modulus under tensile perpendicular to grain have the largest discreteness for bamboo scrimber. From the point of CHV values, the relationship among the mechanical parameters for bamboo scrimber were proposed based on the test results. Compared with other green building materials, bamboo scrimber manufactured based on a new technique has better mechanical performance and could be used in construction area. Three stress strain relationship models which are four-linear model, quadratic function model, and cubic function model were proposed for bamboo scrimber specimens manufactured based on a new technique. The latter two models gives better prediction for stress strain relationship in elastic plastic stage.

Keywords: Bamboo scrimber; parallel to grain; perpendicular to grain; stress–strain relationship model

1 Introduction

Green building materials such as timber [1,2], bamboo [3-6] have attracted more and more scientists' interests. Many engineered bamboo products [7-11] were invented. Bamboo scrimber [11,12] is one of the main engineered bamboo products in the markets recently. There are two main manufacturing methods for bamboo scrimber [12-14] which are cold press technology and hot press technology.

More and more scientists are interested in researching on bamboo scrimber both for the manufacturing technology and mechanical properties. He et al. [15] investigated the mechanical performance of bamboo scrimber made from moso bamboo (*Pyllostachys pubescens*) treated by heat oil. Naresworo Nugroho et al. [16,17] chosen zephyr strand from moso bamboo (*Pyllostachys pubescens* Mazel) to made the structural composite board. Huang [18] examined how the accelerated aging method and aging resistant influence the performance of bamboo scrimber. The physical and mechanical properties of bamboo scrimber have been studied by Ahmad et al. [19]. Pannipa et al. [20] examined the physical and mechanical properties of bamboo scrimber made from an Asian bamboo (*Dendrocalamus asper* Backer).

Sharma et al. [21] compared the mechanical properties for bamboo scrimber with that for laminated bamboo lumbers. Huang et al. [22] and Zhou et al. [23] also investigated the failure mechanisms for bamboo scrimber. Considering the elevated temperatures, Xu et al. [24] examined the compressive and tensile properties of PBSL. Li et al. [11,25] investigated the eccentric compression properties of bamboo scrimber columns produced both by cold press technology. Zhong et al. [26] studied how the temperature influence on the compressive strength parallel to the grain for bamboo scrimber. Wei et al. [27] investigated the properties for bamboo scrimber beams. Zhang et al. [28] studied the mechanical properties of AFRP bamboo scrimber beams.

The former studies are mainly on the bamboo scrimber made by the cold press method, however hot press technology becomes more and more popular. Considering the bamboo bundle preparation, glue immersion, forming and hot pressing process, the manufacturing technology for bamboo scrimber were studied by Liang Cheng [29]. Yu et al. [30] carried out an experimental study on the preparation, physical, mechanical, and interfacial morphological properties of bamboo scrimber. Shangguan et al. [31] investigated the compressive performance of bamboo scrimber and proposed strength models. Li et al. [32] investigated the compression properties of bamboo scrimber manufactured by hot press technology and proposed a stress strain relationship model. As for the stress strain relationship model under compression, Huang et al. [22] also proposed one for bamboo scrimber made by the cold press method.

As discussed above, even though both the manufacturing technology and mechanical properties for bamboo scrimber have been investigated considering many influencing factors, the research on mechanical performance of bamboo scrimber manufactured by hot press technology is limit and good constitutive models for bamboo scrimber are not yet available. A systemic study on the mechanical properties and models is needed. The constitutive model is the fundamental theory for the further mechanical properties' study. Thus, this paper perform a study on the mechanical performance and stress strain relationship for bamboo scrimber manufactured based on a new technique.

2 Materials and Test Methods [32]

With the harvest age of 3-4 years, Moso bamboo (*Phyllostachys pubescens*) were chosen from Yichun City in the Jiangxi province. Natural bamboo culms were cut into tubes (Fig. 1a) with the length of 2000 mm. All tubes were cut into 20 mm wide strips (Fig. 1b), and the outer skin (epidermal) and inner cavity layer (pith peripheral) were removed by a planer. All strips were split into bamboo bundles by passing through a roller press crusher. Then these bamboo strand bundles (Fig. 1c) were dried and charred with the temperature of 165°C and the air pressure of 0.3 MPa. Phenol glue was used to manufacture the bamboo scrimber specimens. All treated bamboo bundles were immersed in glue pool (Fig. 1d) and then dried in the air

(a) Bamboo tubes   (b) Bamboo strips   (c) Bamboo strand bundles

(d) Bundles impregnation   (e) Bundles drying   (f) Bundles in moulds

(g) Pressing machine   (h) Bamboo scrimber   (i) Cross-section

Figure 1: Main manufacturing process for bamboo scrimber

(Fig. 1e). Finally the bamboo bundles were put into moulds (Fig. 1f) and these were then pressed into bamboo scrimber by the pressing machine (Fig. 1g). A transverse compression of 10.3 MPa was applied for the blocks under the hot pressing temperature with the value of 160°C. Gross bamboo scrimber boards could be seen from Fig. 1h and the cross section of bamboo scrimber were shown in Fig. 1i.

In order to investigate the tensile, compression, bending and shear properties as well as the stress strain relationship model for bamboo scrimber manufactured based on a new technique, five groups of specimens were manufactured. Each group consisted of 36 identical specimens. The sizes for the compression specimens and bending specimens are 50 mm × 50 mm × 150 mm and 50 mm × 50 mm × 760 mm respectively. The sizes and shape for other specimens could be seen from Fig. 2. As for the naming rules for the specimens, "TS" and "TH" stand for the tensile parallel to grain group and tensile perpendicular to grain group respectively. "CS", "B660" and "SS" stand for the compression group, bending group and shear group respectively. Four side surfaces of the compression specimens were named as A, B, C, D.

Two strain gauges were pasted on each surface for two wide side surfaces of the tensile specimens and four side surfaces of the compression specimens. The test was performed using a microcomputer-controlled electro-hydraulic servo universal testing machine and a Data Acquisition System. The total loading duration is controlled between 6 and 10 min. The load was applied initially through load control in the elastic stage, and then was changed to displacement control before the proportional limit. The frequencies of all strains were 1 values per second. The test was halted until the specimen had sustained significant damage. The final moisture content was 8.22% and the density was 1254 kg/m^3 for bamboo scrimber with the standard deviation and coefficient of variation of 80.4 kg/m^3, 0.064 respectively. Fig. 3 shows the test photos.
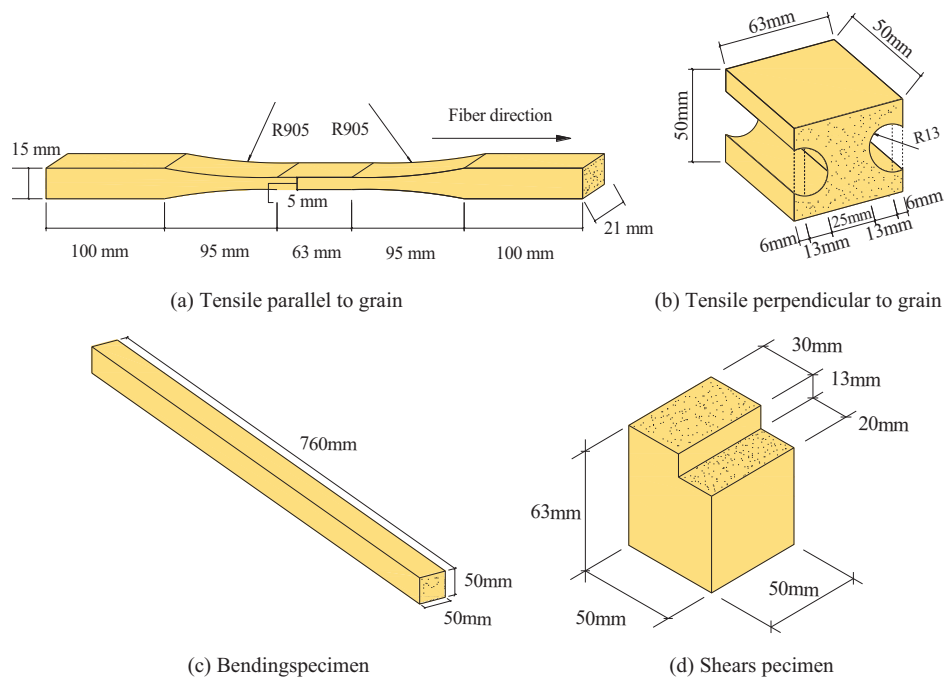
(a) Tensile parallel to grain

(b) Tensile perpendicular to grain

(c) Bendingspecimen

(d) Shears pecimen

Figure 2: Test specimen for bamboo scrimber

(a) Tensile parallel to the strain

(b) Tensile perpendicular to grain

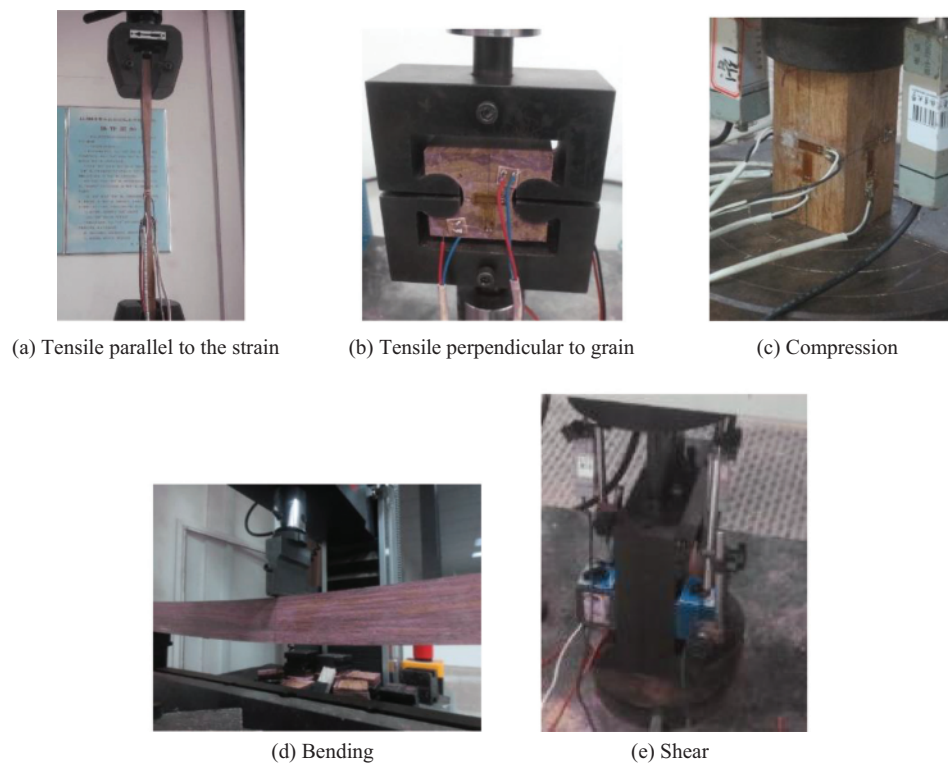(c) Compression

(d) Bending

(e) Shear

Figure 3: Test photos for bamboo scrimber

3 Test Results and Analysis

3.1 Failure Analysis

3.1.1 Tensile Parallel to Grain

Figure 4 shows the stress strain curves for the tensile specimens. Overall speaking, the stress strain curves are linear with the increasing of loading until the final failure. The tensile specimen split suddenly at the ultimate state. None clear crack or failure phenomenon could be seen during the loading process. The slopes for the curves vary among all tensile specimens and it means that the test results for elastic modulus have a certain discreteness.
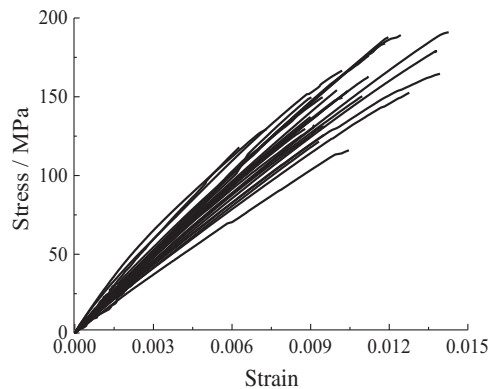

Figure 4: Stress strain curves for tensile specimens parallel to grain

According to the failure process for all specimens, two main failure phenomena series could be classified as can be seen from Fig. 5. The fibers around the natural nodes of bamboo are weak points and the specimens were broken firstly around these points. Detailed failure modes information for tensile specimens can be found in Tab. 1. Most of the specimens failed with the mode A. The total number for mode B is 5 which is 13.89% of 36 specimens. The mean values for strength, elastic modulus and Poisson's ratios for the specimens under tensile parallel to grain are 156.2 MPa, 15649 MPa and 0.441, with the standard deviation of 25.1 MPa, 1586 MPa, 0.055 and with the coefficient of variation of 0.161, 0.101, and 0.124 respectively. The characteristic values for them are 114.9 MPa, 13039 MPa and 0.35 respectively.
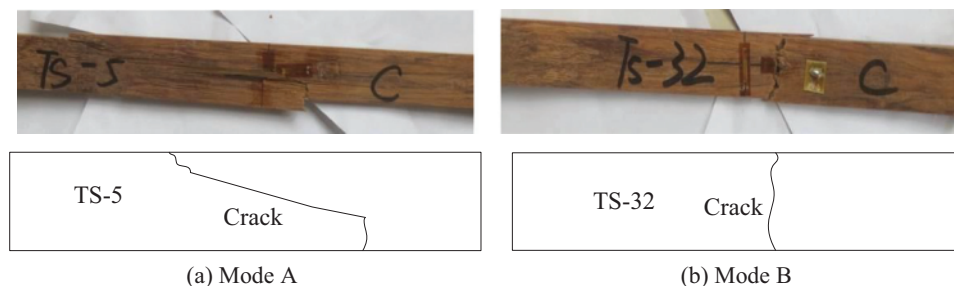

| (a) Mode A | (b) Mode B |

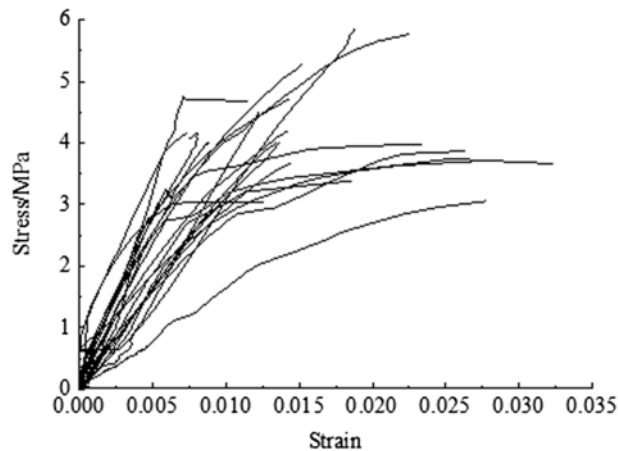**Figure 5:** Typical failure modes for tensile parallel to grain specimens

3.1.2 Tensile Perpendicular to Grain

Figure 6 plots the stress strain relationship for the specimens. Compared with the specimens under tensile parallel to grain, some of the specimens under tensile perpendicular to grain have nonlinear stage

Table 1: Test results for all bamboo scrimber specimens and other materials

		ρ kg/m³	f_{ts} /MPa	E_{ts} /MPa	f_{th} /MPa	E_{th} /MPa	f_{cs} /MPa	E_{cs} /MPa	f_{ch} /MPa	E_{ch} /MPa	f_b /MPa	E_b /GPa	τ_{ss} /MPa
BS [1]	Mean	1254	156.2	15649	3.88	4012	100.9	14160	52.8	4313	144.3	9.919	26.7
	SDV	80.4	25.1	1586	1.11	1032	14.6	1714	9.97	772	12.03	0.766	5.58
	COV	0.064	0.161	0.101	28.64	25.72	0.144	0.121	18.87	17.91	8.34	7.72	20.93
	CHV	1122	114.9	13039	2.05	2314	76.9	11340	36.4	3042	124.5	8.658	17.5
LB [2]	Mean	686	90	–	2	–	77	–	22	–	77–83	11–13	16
BS [3]	Mean	1163	120	–	3	–	86	–	37	–	119	13	15
GLG [4]	Mean	741	143.1	18345	3.2	–	62	32271	5.3	455	122.4	13.26	9.5
GB [5]	Mean	700	83	10344	–	–	42	–	–	–	99	9.407	16
RB [6]	Mean	666	153		–	–	53	–	–	–	135	9	16
LG [7]	Mean	555–625	91.7	11860	–	–	38.3	13070	5.3	1250	90	11.03	–
SS [8]	Mean	383	59	–	–	–	36	–	–	–	67	8	–
DFL [9]	Mean	520	49	–	–	–	57	–	–	–	68	13	–
LBR [10]	Mean										92.6	7999	
LBT [11]	Mean										101.1	9177	

Notes: 1. Present study; 2. Laminated bamboo (Sharma et al.) [21]; 3. Bamboo scrimber (Sharma et al.) [21]; 4. Glued Laminated *Guadua angustifolia Kunth* – tangential (Correal et al.) [8]; 5. GluBam (Xiao et al.) [7,33]; 6. Raw Bamboo *Phyllostachys pubescens* (de Vos.) [34]; 7. *Larix gmelini* (Zhou et al.) [35]; 8. Sitka spruce (Lavers, Kretschmann) [36,37]; 9. Douglas-fir LVL (Kretschmann et al., Clouston et al.) [38,39]; 10. Laminated bamboo lumber under radial bending direction (LBR) (Li et al.) [35]; 11. Laminated bamboo lumber under tangential bending direction (LBT) (Li et al.) [35]; 12. f_{ts} and E_{ts} are the strength and elastic modulus for the specimens under tensile parallel to grain respectively; f_{th} and E_{th} are the strength, and elastic modulus for the specimens under tensile perpendicular to grain; f_{cs} and E_{cs} are the strength and elastic modulus for the specimens under compression parallel to grain respectively; f_{ch}, and E_{ch} are the strength, and elastic modulus for the specimens under compression perpendicular to grain. f_b and E_b are the strength, and elastic modulus for the test specimens under bending; τ_{ss} is the shear strength for the test specimens; COV means coefficient of variation; SDV means the standard deviation; CHV means characteristic value, calculated on the basis that 95% of samples exceed the characteristic value (mean ultimate value – 1.645 × standard deviation).

Figure 6: Stress strain curves for tensile specimens perpendicular to grain

in the stress strain curves. The slope values for the elastic stages have bigger discreteness compare with those for the specimens under tensile parallel to grain. Clear cracks always appeared around the weak points. There are two typical failure models which could be seen from Fig. 7. Seven specimens damaged as mode II. The mean values for strength, and elastic modulus for the specimens under tensile perpendicular to grain are 3.88 MPa and 4012 MPa, with the standard deviation of 1.11 MPa and 1032 MPa, and with the coefficient of variation of 28.64 and 25.72 respectively. The characteristic values for them are 2.05 MPa and 2314 MPa respectively.
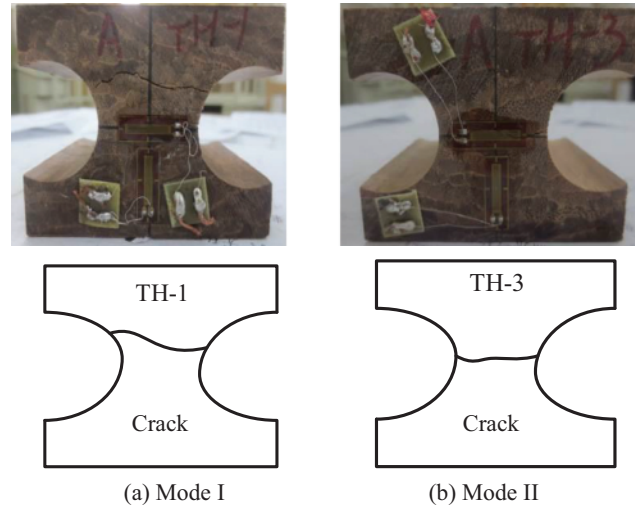

(a) Mode I   (b) Mode II

Figure 7: Typical failure modes for tensile perpendicular to grain specimens

3.1.3 Compression

Figure 8 plots the strain–stress curves for the test specimens under compression both parallel to grain and perpendicular to grain. Compared the two series of the test curves with each other, each specimen experienced elastic stage and elastic-plastic stage. However, the specimens under compression parallel to
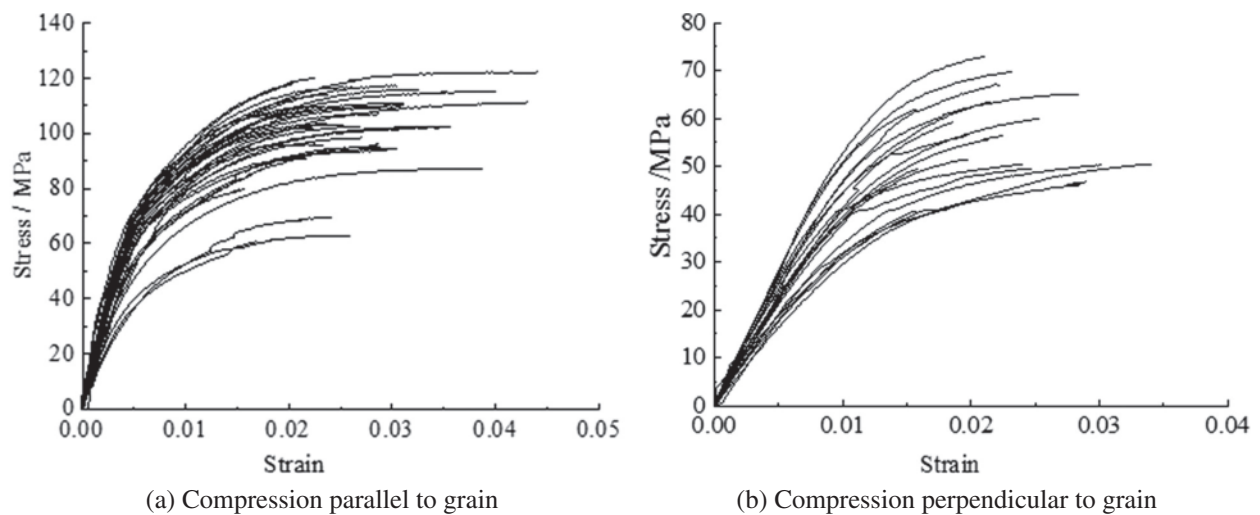

(a) Compression parallel to grain   (b) Compression perpendicular to grain

Figure 8: Stress train curves for compression specimens

grain also had clear plastic stage. According to the final state for the specimens under compression parallel to grain, four typical failure modes could be classified as shown in Fig. 9. 15 specimens damaged with failure mode II which is about 41.67% of all specimens. The mean values for strength, elastic modulus and Poisson's ratios for the specimens under compression parallel to grain are 100.9 MPa, 14160 MPa and 0.403, with the standard deviation of 14.6 MPa, 1714 MPa, 0.039 and with the coefficient of variation of 0.144, 0.121, and 0.098 respectively. The characteristic values for them are 76.9 MPa, 11340 MPa and 0.338 respectively. In addition, the mean values for strength, and elastic modulus for the specimens under compression perpendicular to grain are 52.8 MPa and 4313 MPa, with the standard deviation of 9.97 MPa and 772 MPa, and with the coefficient of variation of 18.87 and 17.91 respectively. The characteristic values for them are 36.4 MPa, and 3042 MPa respectively.

(a) Mode Ⅰ   (b) Mode Ⅱ   (c) Mode Ⅲ   (d) Mode Ⅳ

Figure 9: Typical failure modes for axial compression specimens

3.1.4 Bending

None clear phenomenon could be seen before 80% of the ultimate load. Small cracks appeared in the middle part of the specimens around the ultimate load. With increase of loading, more and more cracks could be seen until the final failure. Fig. 10 shows the typical failure model for bending specimens. The mean values for bending strength and elastic modulus are 144.3 MPa, and 9199 MPa, with the standard deviation of 12.03 MPa and 766 MPa, and with the coefficient of variation of 8.34 and 7.72 respectively. The characteristic values for them are 124.5 MPa and 8658 MPa respectively.
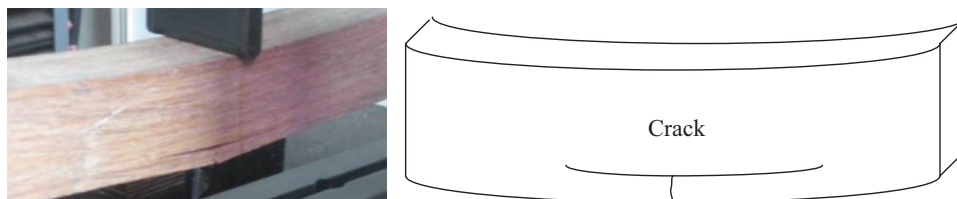

Figure 10: Typical failure mode for bending specimens

3.1.5 Shear

The load displacement curves could be seen in Fig. 11. The discreteness for both the slope values of the curves and the ultimate load values for the specimens is very big. None clear phenomenon could be seen in
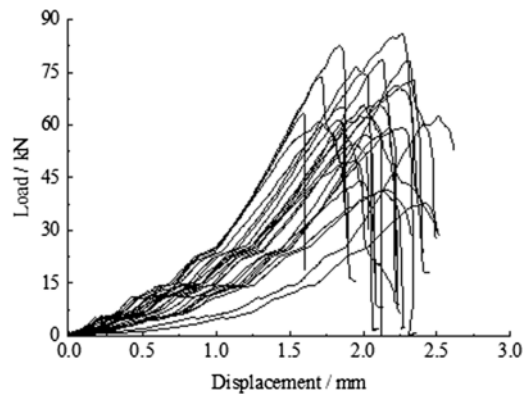
Figure 11: Load displacement curves for shear specimens

the initial stage. Slight noise could be heard around 85% of the ultimate load, and then small cracks could be seen along the main shear line close to the ultimate load. Finally, the specimen split into two main parts and Fig. 12 shows the typical failure model for shear specimens. The mean value for shear strength is 26.7 MPa, with the standard deviation of 5.58 MPa and the coefficient of variation of 20.93. The characteristic value is 17.5 MPa.

Figure 12: Typical failure mode for shear specimens

3.2 Test Results

Table 1 presents the test results for all bamboo scrimber specimens and other results for the materials obtained from literatures. As can be seen from Tab. 1, with the COV values of 28.64 and 25.72 respectively, f_{th} and E_{th} have the largest discreteness among the values for the strength and elastic modulus for bamboo scrimber. Except E_b, all other test values are for bamboo scrimber manufactured based on the new technique are bigger than the test values for bamboo scrimber (Sharma et al.) [21] produced by the traditional method.

The elastic modulus for the bamboo scrimber specimens under tensile parallel to grain is bigger than that for GB and LG but smaller than that for GLG. The elastic modulus for the bamboo scrimber under compression parallel to grain is also smaller than that for GLG but bigger than that for LG. Except the two elastic modulus values mentioned above, all other values for bamboo scrimber specimens are bigger than the corresponding values for other materials listed in Tab. 1. It means that the bamboo scrimber material manufactured based on the new technique mentioned above has very good mechanical properties and could be used in construction area. From the point of CHV values, the relationship among the

mechanical parameters could be expressed as following.

$$\left.\begin{array}{l} f_{ts} = 56f_{th} = 1.5f_{cs} = 3.16f_{ch} = 0.923f_b = 6.56\tau_{ss} \\ E_{ts} = 5.63E_{th} = 1.15E_{cs} = 4.27E_{ch} = 1.51E_b \end{array}\right\} \tag{1}$$

4 Stress Strain Relationship Model

4.1 Four-Linear Model for Stress Strain Relationship

Even though four main stages could be summarized for the whole loading process for bamboo scrimber specimens under compression parallel to grain [32], it is not necessary to consider the descent stage from the design point of view. The elastic modulus value E_{ts} for bamboo scrimber (made of *Phyllostachys pubescens*) under tension parallel to grain is 10.5% bigger than E_{cs} for bamboo scrimber under compression parallel to grain for the mean values. However, the elastic modulus value E_{cs} is 75.9% bigger than E_{ts} for GLG made of *Guadua angustifolia* Kunth. The values for E_{cs} and E_{ts} are not very close to each other for bamboo scrimber made of by every bamboo species. Based on the discussion above, the four-linear model for stress strain relationship was proposed as shown in Fig. 13a. As can be seen from Fig. 13b, the proposed model gives good agreement with the test data.
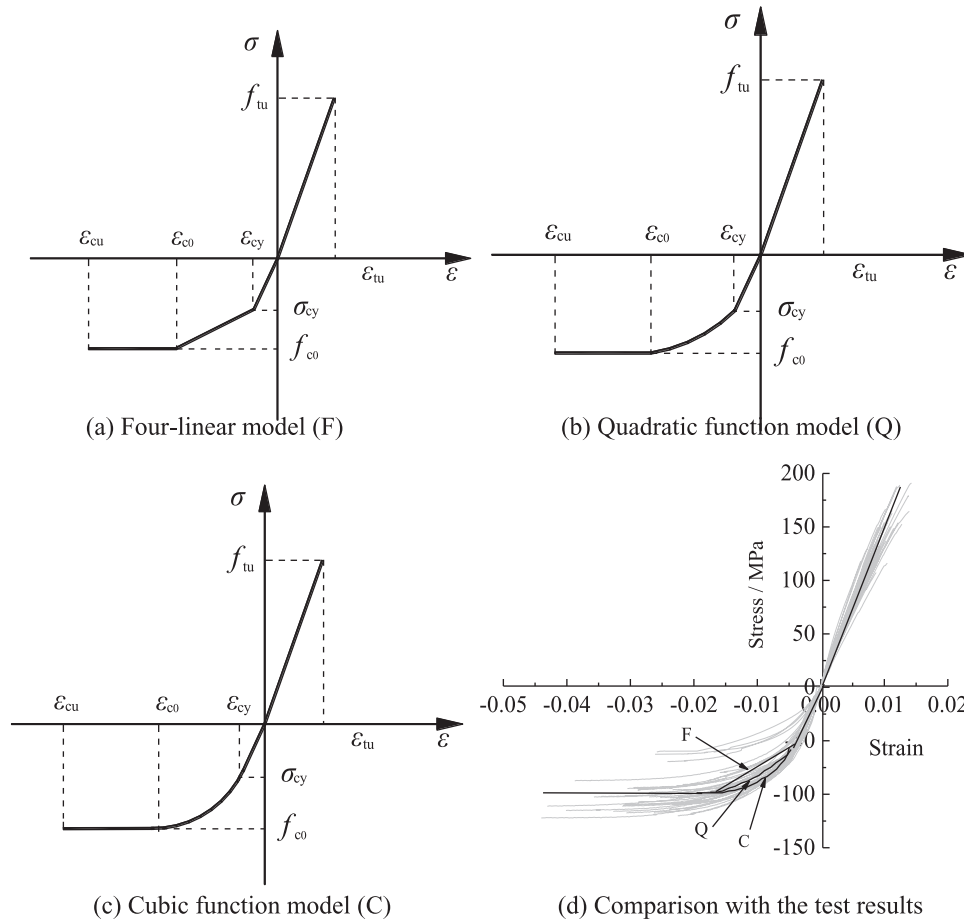

(a) Four-linear model (F)

(b) Quadratic function model (Q)

(c) Cubic function model (C)

(d) Comparison with the test results

Figure 13: Proposed stress strain relationship models

The four-linear stress strain relationship model could be expressed as follows:

$$\sigma = \begin{cases} E_{ts}\varepsilon & (0 \leq \varepsilon \leq \varepsilon_{tu}) \\ E_{cs}\varepsilon & (\varepsilon_{cy} \leq \varepsilon \leq 0) \\ f_{c0}\left[1 - a\left(1 - \dfrac{\varepsilon}{\varepsilon_{c0}}\right)\right] & (\varepsilon_{c0} \leq \varepsilon \leq \varepsilon_{cy}) \\ f_{c0} & (\varepsilon_{cu} \leq \varepsilon \leq \varepsilon_{c0}) \end{cases} \tag{2-1}$$

$$a = \frac{kn-1}{n-1} \tag{2-2}$$

$$n = \frac{\varepsilon_{cy}}{\varepsilon_{c0}} \tag{2-3}$$

$$k = E_c \frac{\varepsilon_{c0}}{f_{c0}} = \frac{E_c}{\dfrac{f_{c0}}{\varepsilon_{c0}}} = \frac{E_c}{E_p} \tag{2-4}$$

where σ is the stress value of the bamboo scrimber under compression parallel to grain; E_{cs} is the modulus of elasticity for bamboo scrimber under compression parallel to grain; E_{ts} is the modulus of elasticity for bamboo scrimber under tensile parallel to grain; E_p is the secant modulus for peak point $(\varepsilon_{c0}, f_{c0})$; ε is the strain value of the PBSL; ε_{cy} is the strain for the yield point; ε_{c0} is the compression peak strain value; f_{c0} is the compression peak stress value; ε_{cu} is the ultimate maximum compression strain value.

4.2 Quadratic Function Model for Stress Strain Relationship

A curve could be chosen for the elastic-plastic stage and the curve could be expressed as the quadratic function [32]. As for other two stages, same lines were chosen as the tri-linear model. This model could be called as quadratic function model for stress strain relationship (Fig. 13b) which is finer than the tri-linear model.

The quadratic function model for stress strain relationship could be expressed as follows:

$$\sigma = \begin{cases} E_{ts}\varepsilon & (0 \leq \varepsilon \leq \varepsilon_{tu}) \\ E_{cs}\varepsilon & (\varepsilon_{cy} \leq \varepsilon \leq 0) \\ f_{c0}\left[1 + a\left(1 - \dfrac{\varepsilon}{\varepsilon_{c0}}\right)^2\right] & (\varepsilon_{c0} \leq \varepsilon \leq \varepsilon_{cy}) \\ f_{c0} & (\varepsilon_{cu} \leq \varepsilon \leq \varepsilon_{c0}) \end{cases} \tag{3-1}$$

$$a = \frac{kn-1}{(n-1)^2} \tag{3-2}$$

$$n = \frac{\varepsilon_{cy}}{\varepsilon_{c0}} \tag{3-3}$$

$$k = E_c \frac{\varepsilon_{c0}}{f_{c0}} = \frac{E_c}{\dfrac{f_{c0}}{\varepsilon_{c0}}} = \frac{E_c}{E_p} \tag{3-4}$$

4.3 Cubic Function Model for Stress Strain Relationship

The curve for the elastic-plastic stage could also be expressed as the cubic function. Thus the cubic function model for stress strain relationship could be chosen which can be seen from Fig. 13c.

The cubic function model for stress strain relationship for bamboo scrimber can be expressed as follows:

$$\sigma = \begin{cases} E_{ts}\varepsilon & (0 \leq \varepsilon \leq \varepsilon_{tu}) \\ E_{cs}\varepsilon & (\varepsilon_{cy} \leq \varepsilon \leq 0) \\ f_{c0}\left[a_0 + a_1\left(\dfrac{\varepsilon}{\varepsilon_{c0}}\right) + a_2\left(\dfrac{\varepsilon}{\varepsilon_{c0}}\right)^2 + a_3\left(\dfrac{\varepsilon}{\varepsilon_{c0}}\right)^3\right] & (\varepsilon_{c0} \leq \varepsilon \leq \varepsilon_{cy}) \\ f_{c0} & (\varepsilon_{cu} \leq \varepsilon \leq \varepsilon_{c0}) \end{cases} \quad (4\text{-}1)$$

$$a_0 = 1 + \frac{2n(kn-1)+(1-n)}{(n-1)^3} \quad (4\text{-}2)$$

$$a_1 = \frac{2n(3-2kn)-k(n+1)}{(n-1)^3} \quad (4\text{-}3)$$

$$a_2 = \frac{(2kn-3)(n+1)+2k}{(n-1)^3} \quad (4\text{-}4)$$

$$a_3 = \frac{2-k(n+1)}{(n-1)^3} \quad (4\text{-}5)$$

$$n = \frac{\varepsilon_{cy}}{\varepsilon_{c0}} \quad (4\text{-}6)$$

$$m = \frac{\sigma_{cy}}{f_{c0}} \quad (4\text{-}7)$$

$$k = E_c\frac{\varepsilon_{c0}}{f_{c0}} = \frac{E_c}{\frac{f_{c0}}{\varepsilon_{c0}}} = \frac{E_c}{E_p} \quad (4\text{-}8)$$

All three proposed models could predict the relationship between the stress and the strain. The main difference is that the latter two models are finer than the tri-linear model (Fig. 13d). In addition, if the values for E_{cs} and E_{ts} are close to each other, the smaller value could be chosen as the elastic modulus both for the tension and compression, and all three models proposed above could be simplified.

5 Conclusions

In order to investigate the basic mechanical properties for bamboo scrimber manufactured based on a new technique, a large quantities of experiments have been carried out. Based on the analysis of the test results, the following conclusions can be drawn.

1. Two main typical failure modes were classified for bamboo scrimber specimens both under tension parallel to grain and tension perpendicular to grain. Brittle failure happened for all tensile tests. The slope values for the elastic stages have bigger discreteness compared with those for the specimens under tensile parallel to grain. The failure modes for bamboo scrimber specimens under compression parallel to grain could be

divided into four. Only one main failure mode happened both for the bending specimens and the shear specimens.

2. With the COV values of 28.64 and 25.72 respectively, f_{th} and E_{th} have the largest discreteness among the values for the strength and elastic modulus for bamboo scrimber. From the point of CHV values, the relationship among the mechanical parameters for bamboo scrimber were proposed based on the test results. Compared with other green building materials, bamboo scrimber manufactured based on a new technique has better mechanical performance and could be used in construction area.

3. Three stress strain relationship models which are four-linear model, quadratic function model, and cubic function model were proposed for bamboo scrimber specimens manufactured based on a new technique. The latter two models gives better prediction for stress strain relationship in elastic plastic stage.

Conflicts of Interest: We declare that we do not have any commercial or associative interest that represents a conflict of interest in connection with the work submitted.

References
1. Wang, Z., Wang, Y. L., Cao, Y., Gao, Z. Z. (2019). Measurements of the shear modulus of materials by the free-plate torsional mode shape method. *Journal of Testing and Evaluation, 47(2),* 1163–1181.
2. Chen, G., Zhou, T., Li, C. L., Zhang, Q., Li, H. (2016). Experimental study on the OSB webbed bamboo beams. *Journal of Nanjing Forestry University (Natural Science Edition), 40(5),* 121–125.
3. Tian, L., Kou, Y., Hao, J. (2019). Axial compressive behaviour of sprayed composite mortar original bamboo composite columns. *Construction and Building Materials, 215,* 726–736. DOI 10.1016/j.conbuildmat.2019.04.234.
4. Hong, C., Li, H., Lorenzo, R., Wu, G., Corbi, I. et al. (2019). Review on connections for original bamboo structures. *Journal of Renewable Materials, 7(8),* 713–730. DOI 10.32604/jrm.2019.07647.
5. Li, Z., He, M., Tao, D., Li, M. (2016). Experimental buckling performance of scrimber composite columns under axial compression. *Composites Part B: Engineering, 86,* 203–213. DOI 10.1016/j.compositesb.2015.10.023.
6. Zhou, N., Zhang, G., Huang, D., Jiang, S., Zhang, Q. (2019). Examination of dynamic characteristics of new bamboo structure by impact hammer test. *Journal of Forestry Engineering, 4(2),* 54–60.
7. Xiao, Y., Yang, R. Z., Shan, B. (2013). Production, environmental impact and mechanical properties of glubam. *Construction and Building Materials, 44(1),* 765–773. DOI 10.1016/j.conbuildmat.2013.03.087.
8. Correal, J. F., Echeverry, J. S., Ramírez, F., Yamín, L. E. (2014). Experimental evaluation of physical and mechanical properties of glued laminated *Guadua angustifolia* Kunth. *Construction and Building Materials, 73,* 105–112. DOI 10.1016/j.conbuildmat.2014.09.056.
9. Li, H., Liu, R., Rodolfo, L., Wu, G., Wang, L. (2019). Eccentric compression properties of laminated bamboo lumber columns with different slenderness ratios. *Proceedings of the Institution of Civil Engineers - Structures and Buildings, 172(5),* 315–326. DOI 10.1680/jstbu.18.00007.
10. Verma, C. S., Chariar, V. M. (2012). Development of layered laminate bamboo composite and their mechanical properties. *Composites Part B: Engineering, 43(3),* 1063–1069. DOI 10.1016/j.compositesb.2011.11.065.

11. Li, H., Su, J., Deeks, A. J., Zhang, Q., Wei, D. et al. (2015). Eccentric compression performance of parallel bamboo strand lumber column. *BioResources, 10(4),* 7065–7080.

12. Fei, B., Liu, R., Liu, X., Chen, X., Zhang, S. (2019). A review of structure and characterization methods of bamboo pits. *Journal of Forestry Engineering, 4(2),* 13–18.

13. Li, Y., Xu, B., Zhang, Q., Jiang, S. (2016). Present situation and the countermeasure analysis of bamboo timber processing industry in China. *Journal of Forestry Engineering, 1(1),* 2–7.

14. Huang, M., Zhang, X., Yu, W., Li, W., Liu, X. (2016). Mechanical properties and structure characterization of bamboo softened by high temperature steam. *Journal of Forestry Engineering, 1(4),* 64–68.

15. He, W., Song, J., Wang, T., Li, J., Xie, L. et al. (2017). Effect of heat oil treatment on bamboo scrimber properties. *Journal of Forestry Engineering, 2(5),* 15–19.

16. Naresworo, N., Naoto, A. (2000). Development of structural composite products made from bamboo I: fundamental properties of bamboo zephyr board. *Journal of Wood Science, 46(1),* 68–74. DOI 10.1007/ BF00779556.

17. Naresworo, N., Naoto, A. (2001). Development of structural composite products made from bamboo II: fundamental properties of laminated bamboo lumber. *Journal of Wood Science, 47(3),* 237–242. DOI 10.1007/ BF01171228.

18. Huang, H. Z. (2009). *The study on accelerated aging method and aging resistant performance of parallel bamboo strand lumber (Master's Thesis).* Nanjing Forestry University, Nanjing, China.

19. Ahmad, M., Kamke, F. A. (2011). Properties of parallel strand lumber from Calcutta bamboo (*Dendrocalamus strictus*). *Wood Science and Technology, 45(1),* 63–72. DOI 10.1007/s00226-010-0308-8.

20. Malanit, P., Barbu, M. C., Frühwald, A. (2011). Physical and mechanical properties of oriented strand lumber made from an Asian bamboo (*Dendrocalamus asper* Backer). *European Journal of Wood and Wood Products, 69(1),* 27–36. DOI 10.1007/s00107-009-0394-1.

21. Sharma, B., Gatóo, A., Bock, M., Ramage, M. (2015). Engineered bamboo for structural applications. *Construction and Building Materials, 81,* 66–73. DOI 10.1016/j.conbuildmat.2015.01.077.

22. Huang, D., Bian, Y., Zhou, A., Sheng, B. (2015). Experimental study on stress-strain relationships and failure mechanisms of parallel strand bamboo made from phyllostachys. *Construction and Building Materials, 77,* 130–138. DOI 10.1016/j.conbuildmat.2014.12.012.

23. Zhou, A. P., Huang, Z. R., Shen, Y. R., Huang, D. S., Xu, J. U. (2018). Experimental investigation of mode-I fracture properties of parallel strand bamboo composite. *Bioresourses, 13(2),* 3905–3921.

24. Xu, M., Cui, Z., Chen, Z., Xiang, J. (2017). Experimental study on compressive and tensile properties of a bamboo scrimber at elevated temperatures. *Construction and Building Materials, 151,* 732–741. DOI 10.1016/j. conbuildmat.2017.06.128.

25. Li, H., Qiu, Z., Wu, G., Ottavia, C., Wei, D. et al. (2019). Slenderness ratio effect on eccentric compression performance of parallel strand bamboo lumber columns. *Journal of Structural Engineering ASCE, 145(8),* 04019077. DOI 10.1061/(ASCE)ST.1943-541X.0002372.

26. Zhong, Y., Wu, G., Ren, H., Jiang, Z. (2017). Bending properties evaluation of newly designed reinforced bamboo scrimber composite beams. *Construction and Building Materials, 143,* 61–70. DOI 10.1016/j. conbuildmat.2017.03.052.

27. Wei, Y., Wu, G., Zhang, Q. S., Jiang, S. X. (2012). Theoretical analysis and experimental test of full-scale bamboo scrimber flexural components. *Journal of Civil, Architectural & Environmental Engineering, 34,* 140–145.

28. Zhang, H., Li, H., Corbi, I., Corbi, O., Wu, G. et al. (2018). AFRP influence on parallel bamboo strand lumber beams. *Sensors, 18(9),* 2854. DOI 10.3390/s18092854.

29. Liang, C. (2009). *Manufacturing Technology of Reconstituted Bamboo Lumber (Master's Thesis).* Inner Mongolia Agricultural University, Huhehaote, China.

30. Yu, Y., Liu, R., Huang, Y., Meng, F., Yu, W. (2017). Preparation, physical, mechanical, and interfacial morphological properties of engineered bamboo scrimber. *Construction and Building Materials, 157,* 1032–1039. DOI 10.1016/j.conbuildmat.2017.09.185.

31. Shangguan, W., Zhong, Y., Xing, X., Zhao, R., Ren, H. (2015). Strength models of bamboo scrimber for compressive properties. *Journal of Wood Science, 61(2),* 120–127. DOI 10.1007/s10086-014-1444-9.

32. Li, H., Qiu, Z., Wu, G., Wei, D., Rodolfo, L. et al. (2019). Compression behaviors of parallel bamboo strand lumber under static loading. *Journal of Renewable Materials, 7(7),* 583–600. DOI 10.32604/jrm.2019.07592.

33. Xiao, Y., Shan, B. (2013). *Modern bamboo structures*. Beijing: China Building Industry Press.

34. de Vos, V. (2010). *Bamboo for exterior joinery: a research in material properties and market perspectives (Thesis)*. Larenstein University, Leeuwarden, Netherlands.

35. Zhou, J., Feng, X., Zhou, X. (2016). Experimental research on mechanical properties of larch glulam. *Journal of Central South University of Forestry & Technology, 36(8),* 125–129, 135.

36. Lavers, G. M. (2002). *The strength properties of timber. Building Research Establishment (BRE) Report Series,* 3rd edition. London.

37. Kretschmann, D. E. (2010). Mechanical properties of wood. In *Wood Handbook*, *General Technical Report FPL-GTR-190*. U.S. Department of Agriculture, Forest Service, Forest Products Laboratory, Madison, WI, Chapter 5, pp. 5-1–5-46.

38. Kretschmann, D. E., Moody, R. C., Pellerin, R. F., Bendtsen, B. A., Cahill, J. M. et al. (1993). Effect of various proportions of juvenile wood on laminated veneer lumber. *Technical Report FPL-RP-521*. U.S. Department of Agriculture, Forest Service, Forest Products Laboratory, Madison, WI.

39. Clouston, P., Lam, F., Barret, J. D. (1998). Incorporating size effects in the Tasi-Wu strength theory for Douglas-fir laminated veneer. *Wood Science and Technology, 32(3),* 215–226. DOI 10.1007/BF00704844.

40. Li, H., Wu, G., Xiong, Z., Corbi, I., Corbi, O. et al. (2019). Length and orientation direction effect on static bending properties of laminated Moso bamboo. *European Journal of Wood and Wood Products, 77(4),* 547–557. DOI 10.1007/s00107-019-01419-6.